

# Effects of space duty cycle on the characteristics of fiber laser coherent beam combination

Wei Wang (王 炜)<sup>1,2,3</sup>, Qihong Lou (楼祺洪)<sup>1,2\*</sup>, Bing He (何 兵)<sup>1,2</sup>, Jun Zhou (周 军)<sup>1,2</sup>, Zhen Li (李 震)<sup>1,2,3</sup>, Yuhao Xue (薛宇豪)<sup>1,2,3</sup>, and Xia Liu (刘 侠)<sup>1,2,3</sup>

<sup>1</sup>Shanghai Institute of Optics and Fine Mechanics, Chinese Academy of Sciences, Shanghai 201800, China

<sup>2</sup>Shanghai Key Laboratory of All Solid-State Laser and Applied Techniques, Shanghai 201800, China

<sup>3</sup>Graduate University of Chinese Academy of Sciences, Beijing 100049, China

\*E-mail: qhlou@mail.shcnc.ac.cn

Received September 3, 2009

The characteristics of fiber laser coherent beam combination are investigated by using a 2×2 fiber laser array with a self-Fourier cavity. The experimental results show that with a certain output width the power ratio of the center spot is increased with the increase of space duty cycle, meanwhile the number of secondary spots is decreased correspondingly. The results are in agreement with theoretic analysis.

OCIS codes: 140.3510, 140.3298.

doi: 10.3788/COL20100805.0490.

High-average-power lasers with diffraction-limited beam quality are desired by many applications such as cutting, welding, and drilling. Cladding-pumped rare-earth-doped fiber lasers offer an excellent combination of compactness, high efficiency, and very good beam quality<sup>[1]</sup>. Large output power is possible because of the excellent thermal dissipation properties of fibers; up to 6000 W of output power in continuous-wave (CW) mode has been demonstrated in a single transverse mode<sup>[2]</sup>. However, it is very hard to scale the output power with a single-aperture laser system. Dawson *et al.* made a study on the output power of fiber lasers, which showed the maximum output power of fiber lasers with the diffraction limit of 36.6 kW for wide bandwidth and 1.86 kW for narrow bandwidth, respectively<sup>[3]</sup>. Other scaling approaches should be taken into closer consideration. One of the most promising techniques is the well-established coherent beam combining method<sup>[4–9]</sup>. This method has been demonstrated for the coherent beam combination (CBC) of an array of lasers into a single output beam with brightness substantially greater than the individual array elements. In the CBC, however, the far-field intensity distribution is affected by the configuration of laser array, such as the element beam width, the distribution of element beam, and the center distance between adjacent beams.

In this letter, we focus on the element beam width, the center distance between the adjacent beams, and the space duty cycle of laser array that impact on the far-field intensity distribution. We carry on theory analyses and get numerical results. By using self-Fourier transform, we get the phase-locking of four-fiber-laser array in the experiment. Through adjusting the center distance between adjacent fiber lasers, we observe the change of the far-field intensity distribution. As the center distance between adjacent fiber lasers is decreased, the scale of center spot is enlarged.

The distribution of the emitter array is shown in Fig. 1. The emitter array is taken to be an  $N \times M$  rectangular grid of elements with single-element field function  $U_0(x, y) = A_0U(x, y)$ , where  $U(x, y) = \exp[-\frac{(x^2+y^2)}{w_0^2}]$ ,  $A_0$

and  $w_0$  are the amplitude and the waist radius, respectively. In the directions of  $x$  axis and  $y$  axis, the center distance between two adjacent beams are  $d_x$  and  $d_y$ , respectively.

According to Ref. [10], when each of the element beam is in-phase, we get the far-field intensity distribution of the CBC, the expression is

$$I_0(f_x, f_y, z) = \frac{A_0^2}{\lambda^2 z^2} |F\{U(x, y)\}|^2 \times \frac{\sin^2(\pi N d_x f_x)}{\sin^2(\pi d_x f_x)} \frac{\sin^2(\pi M d_y f_y)}{\sin^2(\pi d_y f_y)}, \quad (1)$$

where  $f_x = \frac{x_s}{\lambda z}$ ,  $f_y = \frac{y_s}{\lambda z}$ .  $(x_s, y_s)$  is the coordinates of far-field,  $z$  is the transmission distance,  $\lambda$  is the wavelength, and  $F\{U(x, y)\}$  is written as

$$\begin{aligned} F\{U(x, y)\} &= \iint U(x, y) \times \exp[j2\pi(f_x x_s + f_y y_s)] dx_s dy_s \\ &= \pi w_0^2 \exp[-\pi^2 w_0^2 (f_x^2 + f_y^2)]. \end{aligned}$$

So the expression of the far field intensity distribution is

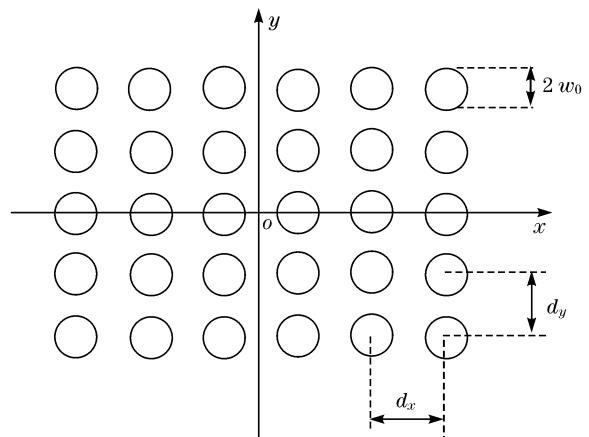


Fig. 1. Two-dimensional (2D) distribution of the emitter array.

rewritten as

$$I_0(f_x, f_y, z) = \frac{\pi^2 w_0^4 A_0^2}{\lambda^2 z^2} \left\{ \exp[-\pi^2 w_0^2 (f_x^2 + f_y^2)] \right\}^2 \times \frac{\sin^2(\pi N d_x f_x)}{\sin^2(\pi d_x f_x)} \frac{\sin^2(\pi M d_y f_y)}{\sin^2(\pi d_y f_y)}. \quad (2)$$

From Eq. (2), the center intensity and the width of the

$$S = \frac{\int_{-1/N}^{1/N} \int_{-1/M}^{1/M} \frac{\pi^2 w_0^4 A_0^2}{d_x d_y \lambda^2 z^2} \left\{ \exp \left[ -\pi^2 w_0^2 \left( \frac{X^2}{d_x^2} + \frac{Y^2}{d_y^2} \right) \right] \right\}^2 \times \frac{\sin^2(\pi N X)}{\sin^2(\pi X)} \frac{\sin^2(\pi M Y)}{\sin^2(\pi Y)} dX dY}{P}, \quad (5)$$

where  $P$  is the total output power of the laser array. From Eqs. (3) and (4), we find that the far-field center intensity is determined by  $A_0$ ,  $z$ ,  $w_0$ ,  $N$ , and  $M$ , and the center distance between two adjacent beams does not influence the far-field center intensity, but it influences the width of the center spot. The width of the center spot increases with the decrease of the center distance between two adjacent beams. In Eq. (5), we find that  $\frac{\pi^2 w_0^4 A_0^2}{d_x d_y \lambda^2 z^2} \left\{ \exp[-\pi^2 w_0^2 (\frac{X^2}{d_x^2} + \frac{Y^2}{d_y^2})] \right\}^2$  increases as the center distance between two adjacent beams decreases, so the power ratio of the center spot  $S$  increases. Figure 2 shows the plots of far-field center-spot power ratio with  $N=2$ ,  $M=2$ ,  $w_0=0.35$  mm.

In this letter, we adopt self-Fourier cavity to get two-dimensional (2D) four-laser array phase locked<sup>[11]</sup>. Two pairs of prisms were used in the experimental setup to change the center distance between adjacent beams. Our experimental setup is illustrated in Fig. 3.

Diode array lasers with emitting wavelength of 975 nm

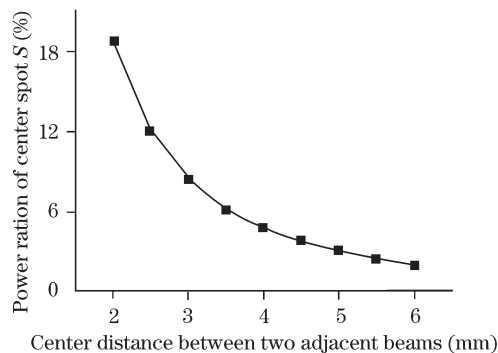


Fig. 2. Power ratio of the center spot versus the center distance between two adjacent beams.

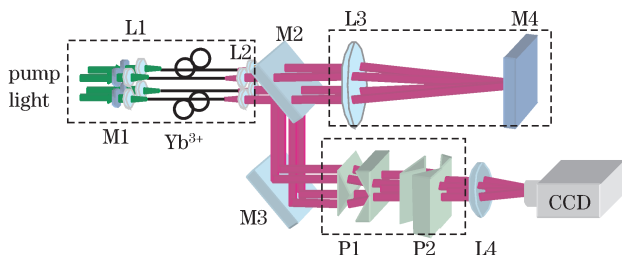


Fig. 3. Schematic diagram of experimental setup. CCD: charge-coupled device.

center spot can be gotten as

$$I_{\text{center}}(f_x, f_y, z) = \frac{\pi^2 A_0^2 w_0^4}{\lambda^2 z^2} N^2 M^2. \quad (3)$$

$$\Delta_x = \frac{2\lambda z}{N d_x}, \quad \Delta_y = \frac{2\lambda z}{M d_y}. \quad (4)$$

We define  $X = f_x d_x$ ,  $Y = f_y d_y$ , so the power ratio of the center spot  $S$  which is the ratio of the center spot power to the total output power is

were used as pump source in the experiment. Pump beams from diode array lasers propagated through four spatial filters (M1) and were coupled into ytterbium-doped double-cladding fibers by using four aspheric lenses (L1), which were end-pumped configuration for the four fiber lasers. The ytterbium-doped double-cladding fibers had a core diameter of 9  $\mu\text{m}$  and a rectangle shape inner cladding size of  $330 \times 170$  ( $\mu\text{m}$ ). The nominal numerical aperture (NA) was 0.1 for the core and 0.47 for the inner cladding. The parameter of M1 was high reflectivity of  $> 99.8\%$  for 1080–1150 nm and high transmission of  $\sim 95\%$  for 975 nm. Four identical plano-convex lenses (L2) were set on the output end of fibers as the collimators. The distribution of lasers array beams was  $2 \times 2$ . The diameter of L2 with a focal length of 6.3 mm was 4 mm. The center distance between collimated beams were  $d_x=4.3$  mm and  $d_y=4.3$  mm, respectively. The collimated beams were placed symmetrically about the resonator optical axis on the front focal plane of the Fourier transform lens (L3) with a focal length of 500 mm. A flat mirror (M4) with  $> 98\%$  reflectivity for 1080–1150 nm was set on the back focal plane of L3. Along the horizontal and vertical directions, we placed two platinum wires with 20- $\mu\text{m}$  diameter in front of M4 to create higher loss for the out-of-phase mode. A beam splitting prism (M2) and a flat mirror (M3) were placed in front of L3, so that the coherent beams output from the M3. P1 and P2 were two pairs of prisms both consisting of isosceles-prism and V-shape prism. P1 and P2 were placed mutually perpendicular in the system.

We examined the beam profile of the output beams using a lens (L4) with a focal length of 30 mm, a CHOU4810 charge-coupled device (CCD) camera, and a laser beam analyzer (LBA-PC300; soft version 3.23; Spiricon Inc.).

Table 1. Power Ratio of Center Spot Versus the Center Distance of Adjacent Beams

| $d_H$ (mm) | $d_V$ (mm) | Power Ratio of the Center Spot (%) |             |
|------------|------------|------------------------------------|-------------|
|            |            | Experiment                         | Calculation |
| 2.47       | 2.87       | 3.62                               | 5.60        |
| 2.45       | 2.91       | 3.42                               | 5.40        |
| 3.46       | 3.18       | 3.22                               | 3.70        |
| 3.56       | 3.36       | 2.91                               | 3.40        |
| 3.95       | 3.96       | 2.57                               | 2.60        |

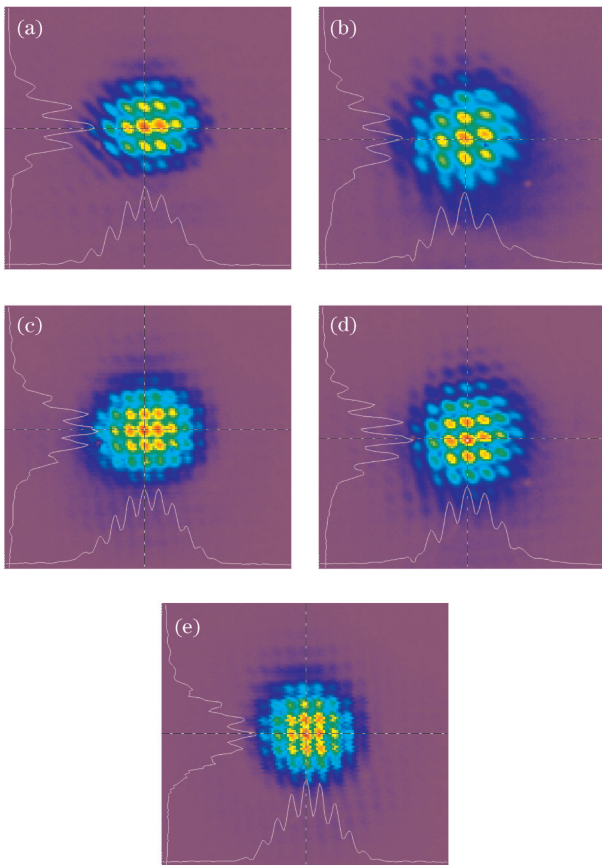


Fig. 4. Far-field intensity distribution of phase-locked laser array. (a)  $d_H=2.47$  mm,  $d_V=2.87$  mm; (b)  $d_H=2.45$  mm,  $d_V=2.91$  mm; (c)  $d_H=3.46$  mm,  $d_V=3.18$  mm; (d)  $d_H=3.56$  mm,  $d_V=3.36$  mm; (e)  $d_H=3.95$  mm,  $d_V=3.98$  mm.

The output powers of single beam were 300, 305, 340, and 320 mW, respectively, and the width of single beam was about 0.7 mm. Through changing the distance between the isosceles-prism and the V-shape prism in P1 and P2, respectively, we could change the center distance between the adjacent beams, and we observed that the far-field beam profile changed, as shown in Fig. 4. We calculated the center power ratio of the center spot with different center distances between the adjacent beams, and compared the results with the experiment results, as given in Table 1.

Figure 4 shows that the width of center spot increases and the number of spots decreases as the center distance between adjacent beams decreases, but the width of out-

put beams does not change. This is because the width of single beam of lasers array does not change. In Table 1, as the center distance between adjacent beams increases from 2.47 to 3.95 mm in horizontal direction ( $d_H$ ) and from 2.87 to 3.96 mm in vertical direction ( $d_V$ ), respectively, the experimental power ratio of the center spot decreases from 3.62% to 2.57%, and the numerical power ratio of the center spot decreases from 5.6% to 2.6%. The above analysis is demonstrated in Fig. 4 and Table 1.

In this letter, when the laser array is given and the width of single beam is defined, we analyze the effects of the center distance between adjacent beams on the CBC. Experiment is done to demonstrate our analysis. It is shown that increasing the space duty cycle of laser array increases the power ratio of the center spot at the far-field and enlarges the area of the center spot, but the far-field center-intensity does not change correspondingly.

This work was supported by the National "863" Program of China (No. 2008AA03Z405) and the Shanghai Rising-Star Program (No. 09QB1401700).

## References

1. L. Michaille, C. R. Bennett, D. M. Taylor, and T. J. Shepherd, *IEEE J. Sel. Top. Quantum Electron.* **15**, 328 (2009).
2. D. Gapontsev, in *Solid State and Diode Laser Technology Review Technical Digest* 258 (2008).
3. J. W. Dawson, M. J. Messerly, R. J. Beach, M. Y. Shverdin, E. A. Stappaerts, A. K. Sridhran, P. H. Pax, J. E. Heebner, C. W. Siders, and C. P. J. Barty, *Opt. Express* **16**, 13240 (2008).
4. J. Lhermite, A. Desfarges-Berthelemot, V. Kermene, and A. Barthelemy, *Opt. Lett.* **32**, 1842 (2007).
5. T. H. Loftus, A. M. Thomas, M. Norsen, J. D. Minelly, P. Jones, E. Honea, S. A. Shakir, S. Hendow, W. Culver, B. Nelson, and M. Fitelson, in *Proceedings of the Advanced Solid-State Photonics WA4* (2007).
6. C. J. Corcoran and K. A. Pasch, *J. Opt. A: Pure Appl. Opt.* **7**, L1 (2004).
7. C. J. Corcoran and F. Durville, *Appl. Phys. Lett.* **86**, 201118 (2005).
8. P. Zhou, Z. Liu, X. Xu, X. Wang, X. Li, and Z. Chen, *Chin. Opt. Lett.* **6**, 625 (2008).
9. P. Zhou, Z. Chen, X. Wang, X. Li, Z. Liu, X. Xu, J. Hou, and Z. Jiang, *Chin. Opt. Lett.* **6**, 523 (2008).
10. C. D. Nabors, *Appl. Opt.* **33**, 2284 (1994).
11. B. He, Q. Lou, J. Zhou, J. Dong, Y. Wei, D. Xue, Y. Qi, I. Su, L. Li, and F. Zhang, *Opt. Express* **14**, 2721 (2006).